Nano Today 49 (2023) 101793

Contents lists available at ScienceDirect

Nano Today

journal homepage: www.elsevier.com/locate/nanotoday

Manipulation of hydrophobic motifs and optimization of sequence patterns to design high stability peptides against piglet bacterial infections

Peng Tan [a,1], Zhihong Sun [b,1], Qi Tang [a], Shenrui Xu [a], Tao Wang [c], Yakun Ding [d], Huiyang Fu [a], Chenlong Zhou [a], Yucheng Zhang [a], Zitian Yue [a], Xi Ma [a,e,*]

[a] State Key Laboratory of Animal Nutrition, College of Animal Science and Technology, China Agricultural University, Beijing, China
[b] Laboratory for Bio-Feed and Molecular Nutrition, Department of Animal Science and Technology, Southwest University, Chongqing, China
[c] Luoyang Key Laboratory of Animal Genetic and Breeding, College of Animal Science, Henan University of Science and Technology, Luoyang, China
[d] Henan International Joint Laboratory of Crop Gene Resource and Improvements, School of Agricultural Sciences, Zhengzhou University, Zhengzhou, China
[e] Beijing Jingwa Agricultural Science & Technology Innovation Center, Beijing, China

ARTICLE INFO

Article history:
Received 24 September 2022
Received in revised form 6 January 2023
Accepted 17 February 2023
Available online xxxx

Keywords:
Antibacterial biomaterials
High stability
Manipulation of hydrophobic motifs
Optimization of sequence patterns
In vivo efficacy

ABSTRACT

The risk of resistance to traditional antibiotics has led to a shift in attention to novel antimicrobial functional biomaterials. Antimicrobial peptides (AMPs) have been recognized since the date of birth as a powerful candidate for antibiotic replacement materials. However, immature salt and protease stability, as well as systemic toxicity, hinder the translation of AMPs from the bench to the bedside. Herein, the original motif $(KP)_3(HYXP)_n(KP)_3$-NH_2 (X = Trp or Phe, Y = Ile or Leu, n = 2, 3, 4, 5, or 6) was designed based on the principles of manipulating hydrophobic motifs, optimizing sequence patterns, as well as circumventing cleavage sites of proteases. Original motif was derived a 20-member library for obtaining AMPs with excellent antimicrobial activity, high salt, and protease stability. Results indicated that the target peptides HLFP-5 and HLWP-4 obtained using a comprehensive and integrated screening process exhibited excellent antibacterial ability, salts stability, and protease stability. Membrane cleavage and cell cycle interference-dominated mechanisms of action make target peptides less susceptible to drug resistance than antibiotics. Additionally, advanced target peptides HLFP-5 and HLWP-4 were able to exert direct antimicrobial efficacy *in vivo* to treat piglets with a systemic bacterial infection. Collectively, these findings may provide novel insights for future design principles, and help drive the application of antibacterial biomaterials in animal husbandry for replacing antibiotics.

Introduction

Due to the frequent occurrence of intractable infections caused by antibiotic resistance worldwide, there is an urgent need to develop novel alternative medicines or immunomodulatory strategies [1–6]. Furthermore, in recent years, Chinese government has completely prohibited the addition of growth promoting antibiotics to feed, which has led to a great increase in the demand for alternatives to antibiotics in animal husbandry. As a biomaterial, antimicrobial peptides (AMPs), which are characterized by broad-spectrum antibacterial activity, excellent biocompatibility, and not easy to generate drug resistance, have been regarded as one of the ideal alternatives to antibiotics since their birth. Moreover, most the AMPs induce bacterial death by disturbing the structure of the bacterial membrane, which is different from antibiotics acting on specific targets. Therefore, AMPs are more promising to deal with multidrug-resistant bacteria.

Although AMPs show great advantages in combating drug-resistant bacteria, at present, the AMPs entering the clinical stage are very limited, one of the important reasons is that their protease hydrolysis stability and salt stability are not mature [7–10]. To solve this problem, a large number of researchers have devoted their efforts to the development of peptidomimetic [11], peptide-based nanomaterials [12,13], peptide polymers [14], lipopeptide [15], and chemical modification strategies [16], however, genetic engineering

* Corresponding author at: State Key Laboratory of Animal Nutrition, College of Animal Science and Technology, China Agricultural University, Beijing, China.
E-mail address: maxi@cau.edu.cn (X. Ma).
[1] These authors contributed equally to this work.

https://doi.org/10.1016/j.nantod.2023.101793
1748-0132/

systems cannot produce the above-mentioned modified peptides due to the incorporation of non-natural substances, limiting the possibility of inexpensive production of applicable AMPs. Combinatorial arrays of cationic and hydrophobic groups composed of natural amino acids offer endless possibilities and are ideal for addressing proteolytic and salt stability of AMPs. Therefore, we intend a logic-based strategy to design economically feasible, easily synthesized, and simultaneously protease and salt stable AMP templates.

The gradual clarification of the structure-function relationships of AMPs provides support for the exploration of peptide-based biomaterials with high proteolytic stability and salt stability. We have long been committed to studying the stability and structure-active relationships of peptide-based biomaterials [17,18]. Based on previous studies, we found that the rearrangement of amino acids is difficult to simultaneously overcome the weak proteolytic stability and salt stability, and may disrupt the parameter balance of AMPs, causing AMPs to lose broad-spectrum antimicrobial activity or increase their cytotoxicity [19]. Herein, to overcome these difficulties, we tried to simplify sequence templates, circumvent cleavage sites, and manipulate the hydrophilic/hydrophobic balance to design a series of peptides with high salt stability and protease hydrolysis stability, mainly including the following design principles: i) Aromatic amino acids were chosen as the hydrophobic core of the peptide chain (X = Trp or Phe), which enabled the peptide to insert deeply and firmly into the bacterial membrane, which was beneficial to induce membrane perturbation [20]. Additionally, the bulky aromatic ring has a high membrane interface affinity, which can reduce the salt sensitivity of AMPs [21]. ii) Proline (Pro) is located at the C-terminus of the aromatic amino acids, preventing chymotrypsin from cleaving the C-terminus of the aromatic amino acids and preventing pepsin from cleaving the N-terminus of the aromatic amino acids. [19]. iii) Place an aliphatic hydrophobic amino acid (Y=Ile or Leu) at the N-terminus of the aromatic amino acid to further increase the hydrophobicity and the depth of the polar face of the peptide chain [22]. When aliphatic amino acid is Leu, Pro at the N-terminal of His and Pro at the C-terminal of aromatic amino acid limit the cleavage of Leu by pepsin. iv) Histidine (His) is placed at the N-terminus of the aliphatic hydrophobic amino acid (Ile or Leu) to prevent pepsin cleaving the C-terminus of the aromatic amino acid (Trp or Phe)[23]. v) Lysines (Lys) are located at both ends of the sequence as cationic amino acids, providing a positive charge to the sequence to provide the necessary driving force for the interaction of peptides with bacteria. At the same time, a Pro was placed at the C-terminus of each Lys to prevent cleavage by trypsin. vi) The C-terminus of the peptide was aminated to further enhance antibacterial activity and improve stability. Based on the above design principles, and repeated for the hydrophobic region, we generated an engineered peptide library $(KP)_3(HYXP)_n(KP)_3$-NH_2 (X = Trp or Phe, Y=Ile or Leu, n = 2, 3, 4, 5, or 6) (Fig. 1a, b), and deduced 20 AMPs (Table 1). In this study, our purpose was to develop an AMP composed of natural amino acids with high proteolysis and salt stability and study its antibacterial activity, stability, and bactericidal mechanism, and evaluate its application value by using a piglet infection model (Fig. 1c–e).

Results and discussion

Design and structural characterization of peptides

Sufficient positive charge and hydrophobicity are necessary conditions for most AMPs to exert antibacterial activity. In this study, Lys was chosen as the positively charged amino acid, and the number was used as six, because studies have shown that the activity of AMPs with more than six positive charges will no longer increase and there is a risk of loss of biocompatibility [24]. Furthermore, a combination of aromatic and aliphatic amino acids was adopted in the selection of hydrophobic amino acids, because although the protease stability of aromatic amino acids is not as good as that of aliphatic amino acids, their membrane disruption ability is stronger, to ensure that the peptides have strong broad-spectrum antibacterial activity. All peptides were prepared using standard solid-phase synthesis, purified by reversed-phase high-performance liquid chromatography (RP-HPLC), and the molecular weight of the peptides was determined by matrix-assisted laser desorption/ionization time-of-flight mass spectrometry (MALDI-TOF-MS). The purity of all peptides was above 95 %, and the theoretical relative molecular mass was close to the measured relative molecular mass, indicating that the peptides were successfully synthesized (Fig. S1 and S2).

The secondary structure of the peptide was determined by circular dichroism (CD). PBS was used to simulate an aqueous environment, sodium dodecyl sulfate (SDS) was used to simulate a negatively charged membrane environment, and trifluoroethanol (TFE) was used to simulate a hydrophobic environment. As shown in Fig. 1f, all peptides had a negative peak at wavelength 200–205 nm in PBS, indicating that the peptides exhibited random coil conformation. In SDS, the negative peaks of the peptides shifted to higher wavelengths, but their secondary structures did not change significantly. In TFE, the peptides had a negative peak at 200–205 nm, and most of the peptides had a positive peak at 220–225 nm, especially the positive peak of Trp-rich peptides is more obvious, indicating that the peptides formed a polyproline II helix conformation. Since all peptides contain a large amount of proline, the pyrrole ring of the Pro side chain causes the peptide to form a rigid structure, making the peptide unable to convert into α-helix or β-sheet in the hydrophobic and membrane environment.

In vitro antibacterial activity, toxicity, and stability of peptides

Representative standard Gram-negative and positive strains such as *Escherichia coli* (*E. coli*), and *Staphylococcus aureus* (*S. aureus*) were selected to evaluate the antibacterial activity of the peptides. To more intuitively evaluate the antibacterial ability of the peptides, the minimum inhibitory concentration (MIC) of the peptides was calculated as the geometric means (GMs). As shown in Table 2, among all the engineered peptides, with the increase in the number of repetitions of the hydrophobic unit of the engineered peptide, the antibacterial activity showed a trend of first increasing and then decreasing, indicating that a certain number of hydrophobic amino acid residues are required for the activity of the peptides. However, there is a threshold for the hydrophobicity of peptides beyond which the activity of the peptide no longer increases or even decreases. Therefore, the relationship between hydrophobicity and activity is not linear, proper hydrophobicity is the key to maintaining antibacterial ability, and too high hydrophobicity can hinder the interaction of peptides with bacterial membranes [25]. This phenomenon can be explained by the fact that high hydrophobicity causes peptide self-association, which prevents peptides from passing through the cell wall of prokaryotic cells, therefore, peptides exceeding optimal hydrophobicity tend to exhibit reduced antibacterial activity [26].

An important indicator of clinical translation of AMPs is cytotoxicity. Therefore, the cytotoxicity of the peptides against intestinal porcine epithelial cells (IPEC-1) was evaluated. As shown in Fig. 2b, among all engineered peptides, peptides with less than four hydrophobic unit repeats did not show significant cytotoxicity at 128 μM. Additionally, it can be seen from the results that the cytotoxicity of the peptide is affected by its hydrophobicity, and the hydrophobicity exceeding the threshold will cause severe damage to eukaryotic cells. Specifically, among the hydrophobic amino acids constituting the engineered peptide, Trp is more hydrophobic than Phe, and Ile is more hydrophobic than Leu [27]. Therefore, the

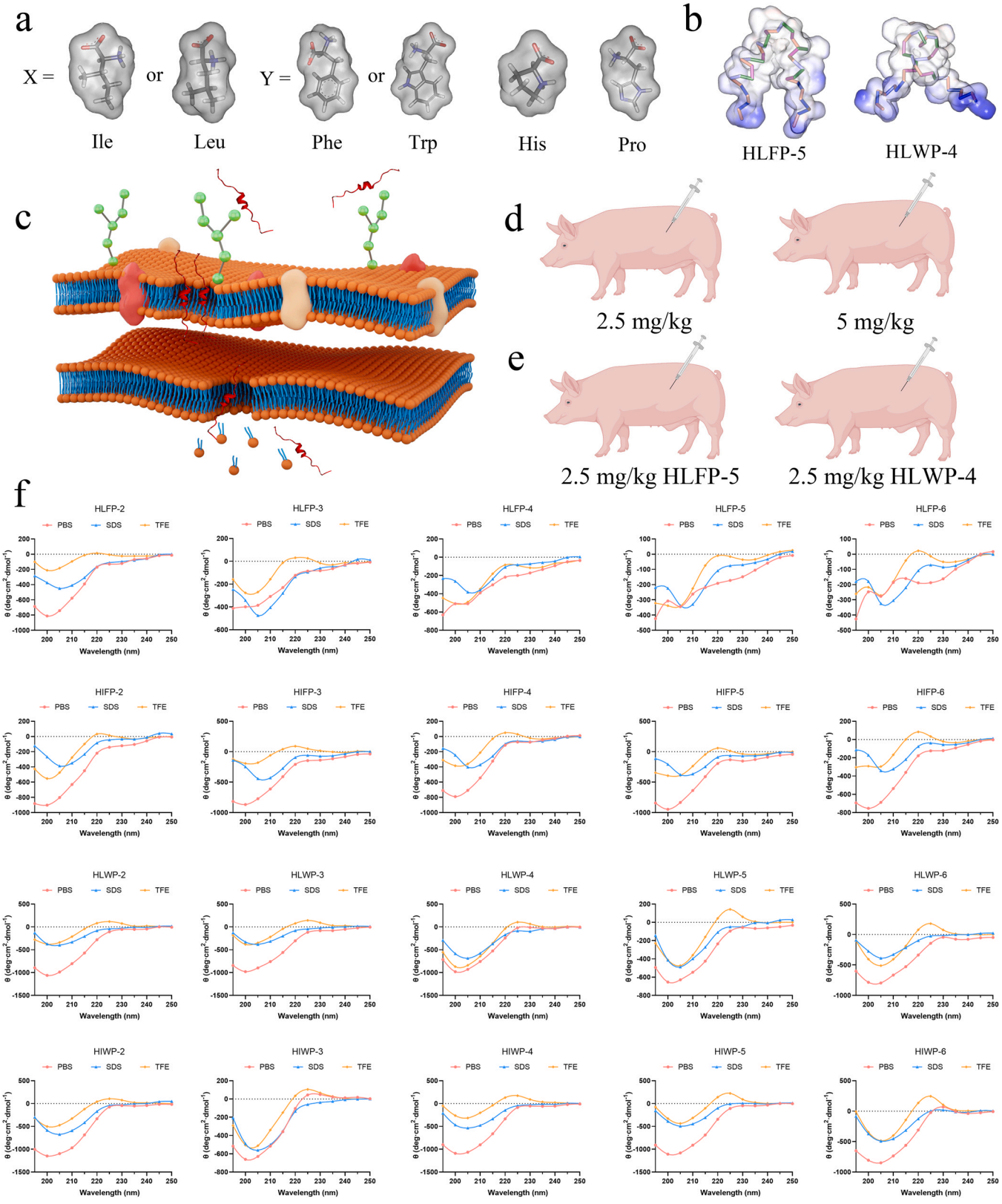

Fig. 1. a) Amino acid composition of highly stability AMPs. b) Skeleton structure of target peptides HLFP-5 and HLWP-4. c) Schematic diagram of the mechanism of action of the target peptides. Adapted with permission from Ref [10]. Copyright 2022, Wiley-VCH. d, e) Schematic diagram of the *in vivo* d) toxicity and e) activity assay flow of target peptides. f) CD spectra of all peptides.

peptide composed of the hydrophobic unit of HIWP exhibits the strongest cytotoxicity, the peptides with more than five repeating units of the hydrophobic unit killed almost all cells at a concentration of 64 μM. Fortunately, among all engineered peptides, the peptides HLFP-4, HLFP-5, HIFP-4, HIFP-5, HLWP-4, and HIWP-4 exhibited excellent broad-spectrum antibacterial activity while

Table 1
Physicochemical parameters of the high stability peptides.

Peptides	Sequence	Theoretical MW	Measured MW[a]	Hydrophobicity[b]	Amino acids
HLFP-2	KPKPKPHLFPHLFPKPKPKP-NH_2	2357.93	2357.92	0.353	20
HLFP-3	KPKPKPHLFPHLFPHLFPKPKPKP-NH_2	2852.51	2852.51	0.475	24
HLFP-4	KPKPKPHLFPHLFPHLFPHLFPKPKPKP-NH_2	3347.10	3347.09	0.562	28
HLFP-5	KPKPKPHLFPHLFPHLFPHLFPHLFPKPKPKP-NH_2	3841.69	3841.68	0.627	32
HLFP-6	KPKPKPHLFPHLFPHLFPHLFPHLFPHLFPKPKPKP-NH_2	4336.27	4336.27	0.678	36
HIFP-2	KPKPKPHIFPHIFPKPKPKP-NH_2	2357.93	2357.92	0.363	20
HIFP-3	KPKPKPHIFPHIFPHIFPKPKPKP-NH_2	2852.51	2852.51	0.488	24
HIFP-4	KPKPKPHIFPHIFPHIFPHIFPKPKPKP-NH_2	3347.10	3347.09	0.576	28
HIFP-5	KPKPKPHIFPHIFPHIFPHIFPHIFPKPKPKP-NH_2	3841.69	3841.68	0.643	32
HIFP-6	KPKPKPHIFPHIFPHIFPHIFPHIFPHIFPKPKPKP-NH_2	4336.27	4336.27	0.695	36
HLWP-2	KPKPKPHLWPHLWPKPKPKP-NH_2	2436.00	2435.99	0.399	20
HLWP-3	KPKPKPHLWPHLWPHLWPKPKPKP-NH_2	2969.62	2969.62	0.533	24
HLWP-4	KPKPKPHLWPHLWPHLWPHLWPKPKPKP-NH_2	3503.24	3503.24	0.628	28
HLWP-5	KPKPKPHLWPHLWPHLWPHLWPHLWPKPKPKP-NH_2	4036.87	4036.86	0.699	32
HLWP-6	KPKPKPHLWPHLWPHLWPHLWPHLWPHLWPKPKPKP-NH_2	4570.49	4570.48	0.755	36
HIWP-2	KPKPKPHIWPHIWPKPKPKP-NH_2	2436.00	2435.99	0.409	20
HIWP-3	KPKPKPHIWPHIWPHIWPKPKPKP-NH_2	2969.62	2969.62	0.545	24
HIWP-4	KPKPKPHIWPHIWPHIWPHIWPKPKPKP-NH_2	3503.24	3503.24	0.642	28
HIWP-5	KPKPKPHIWPHIWPHIWPHIWPHIWPKPKPKP-NH_2	4036.87	4036.86	0.715	32
HIWP-6	KPKPKPHIWPHIWPHIWPHIWPHIWPHIWPKPKPKP-NH_2	4570.49	4570.48	0.772	36

[a] Measured molecular weight was identified by MALDI-TOF MS.
[b] Hydrophobicity (H) values means the total hydrophobicity (sum of all residue hydrophobicity indices) divided by the number of residues, and they were calculated from https://heliquest.ipmc.cnrs.fr/cgi-bin/ComputParams.py.

maintaining low cytotoxicity. A theory that can explain this phenomenon is that there are differences in the membrane structure of prokaryotic cells and eukaryotic cells, for prokaryotic cells, most of the anionic components in the membrane face the membrane surface, which is conducive to electrostatic interaction with peptides, on the contrary, for eukaryotic cells, most of the anionic components in the membrane are oriented towards the interior [28]. Therefore, the above engineered peptides can selectively inhibit bacterial growth without destroying eukaryotic cells.

Stability is a key parameter that determines the therapeutic efficacy of AMPs *in vivo*. According to previous reports, the presence of cations affects the antimicrobial activity of AMPs [29]. Salts in the physiological environment will weaken the binding ability between the peptide and the membrane, leading to reduced efficacy of peptides. Furthermore, the salts can also bind to the negatively charged components to enhance the rigidity of the bacterial membranes [30,31]. As shown in Fig. 2a, Na^+ and Mg^{2+} had the greatest impact on the antibacterial activity of engineered peptides, and the peptides HLFP-4 and HIFP-4 completely lost their activity in the presence of Na^+. In a physiological environment, other salt concentrations are lower, thus having little or no effect on the antibacterial ability of the peptides [32]. Furthermore, the results show that the salt stability order of the peptides is HIWP-4 > HIFP-4, HLWP-4 > HLFP-4, which indicates that although the aromatic rings of Phe and Trp are beneficial to improving the salt stability, Trp is more potent than Phe. This suggests that, on the one hand, an increase in the overall hydrophobicity of AMPs can reduce their salt sensitivity, on the other hand, the indole ring present on the Trp residue can penetrate deeper into the bacterial membrane and increase the membrane-bound area to improve the salt stability of the peptides [33].

Another factor to consider in AMPs design is proteases proteolytic stability [34]. Human or animal endogenous proteases including pepsin, trypsin, and chymotrypsin are major threats to AMPs. It is well known that most AMPs require positive charge and

Table 2
Minimum inhibitory concentration (MIC) of the peptides.

Peptides	MIC (μM)										GM[a]
	E. coli ATCC25922	*E. coli* K88	*E. coli* K99	*S. typhimurim* SL1344	*P. aeruginosa* ATCC27853	*C. rodentium* DBS100	*S. aureus* ATCC6538	*S. aureus* CVCC1882	*S. aureus* 43300	*S. epidermidis* ATCC49134	
HLFP-2	> 64	32	> 64	> 64	> 64	> 64	32	> 64	> 64	> 64	97.01
HLFP-3	32	16	64	> 64	> 64	4	8	32	64	8	27.86
HLFP-4	4	4	2	32	16	2	2	8	16	2	5.28
HLFP-5	2	2	2	4	8	2	2	2	8	2	2.83
HLFP-6	4	2	2	> 64	> 64	2	1	2	4	2	4.92
HIFP-2	> 64	16	64	> 64	> 64	64	64	> 64	> 64	> 64	84.45
HIFP-3	16	8	16	32	> 64	4	2	32	64	8	16.00
HIFP-4	4	2	2	16	16	2	2	8	16	4	4.92
HIFP-5	2	2	2	8	8	1	2	2	8	4	3.03
HIFP-6	2	2	2	8	8	2	2	4	8	2	3.25
HLWP-2	> 64	32	> 64	> 64	> 64	32	8	32	64	32	51.98
HLWP-3	16	16	32	32	> 64	4	2	8	16	4	13.00
HLWP-4	4	2	2	8	16	1	2	4	8	2	3.48
HLWP-5	2	2	2	4	8	1	2	2	4	1	2.30
HLWP-6	4	2	2	> 64	> 64	1	1	1	2	2	4.00
HIWP-2	32	16	64	64	> 64	64	16	64	64	32	45.25
HIWP-3	16	4	8	32	64	4	2	16	32	8	11.31
HIWP-4	2	2	2	4	8	1	2	4	8	2	2.83
HIWP-5	2	2	1	4	4	1	2	2	2	2	2.00
HIWP-6	8	2	2	> 64	> 64	2	2	1	4	2	5.28

[a] GM was calculated as the geometric mean of antimicrobial peptides MICs. When no detectable antibacterial activity was observed at 64 μM, a value of 128 μM was used to calculate the GM.

a

Peptides	*E. coli* ATCC25922									
	Control	NaCl	$MgCl_2$	KCl	NH_4Cl	$ZnCl_2$	$FeCl_3$	Trypsin	Chymotrypsin	Pepsin
HLFP-4	4	>64	32	4	4	8	8	4	4	4
HLFP-5	2	8	4	2	2	2	2	2	2	2
HIFP-4	4	>64	32	4	4	4	4	4	>64	4
HIFP-5	2	8	4	2	2	2	2	2	>64	2
HLWP-4	4	16	16	4	4	4	4	4	4	4
HIWP-4	2	16	8	2	2	4	2	2	>64	2

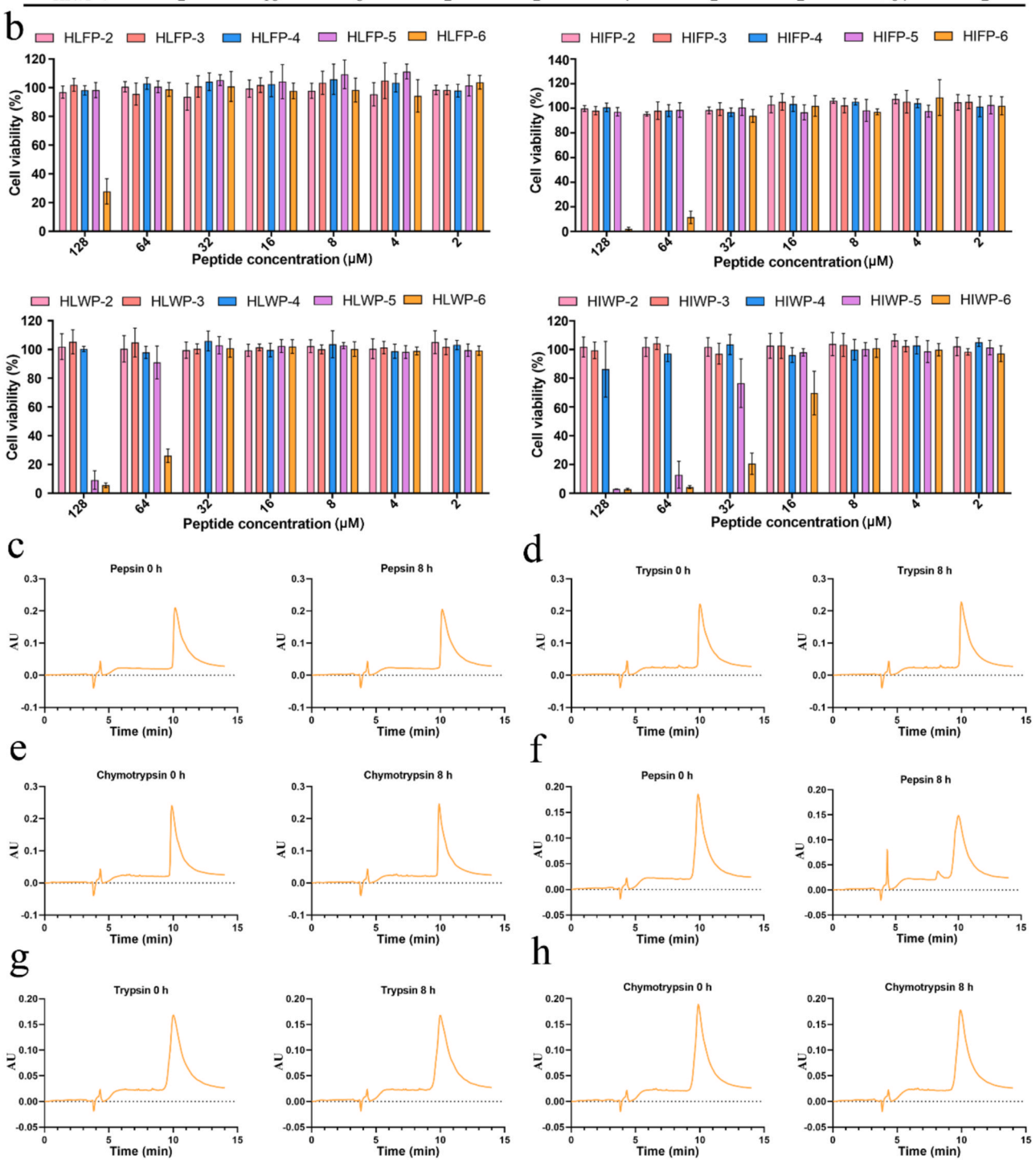

Fig. 2. a) MIC values of peptides HLFP-4, HLFP-5, HIFP-4, HIFP-5, HLWP-4, or HIWP-4 in the presence of physiological salts or proteases (8 mg/mL pepsin, 8 mg/mL trypsin, or 2 mg/mL chymotrypsin). b) Cytotoxicity of the peptides against IPEC-1 cells. c-e) RP-HPLC images of peptide HLFP-5 incubated with c) 8 mg/mL pepsin, d) 8 mg/mL trypsin, or e) 2 mg/mL chymotrypsin for 0 or 8 h. f-h) RP-HPLC images of peptide HLWP-4 incubated with f) 8 mg/mL pepsin, g) 8 mg/mL trypsin, or h) 2 mg/mL chymotrypsin for 0 or 8 h.

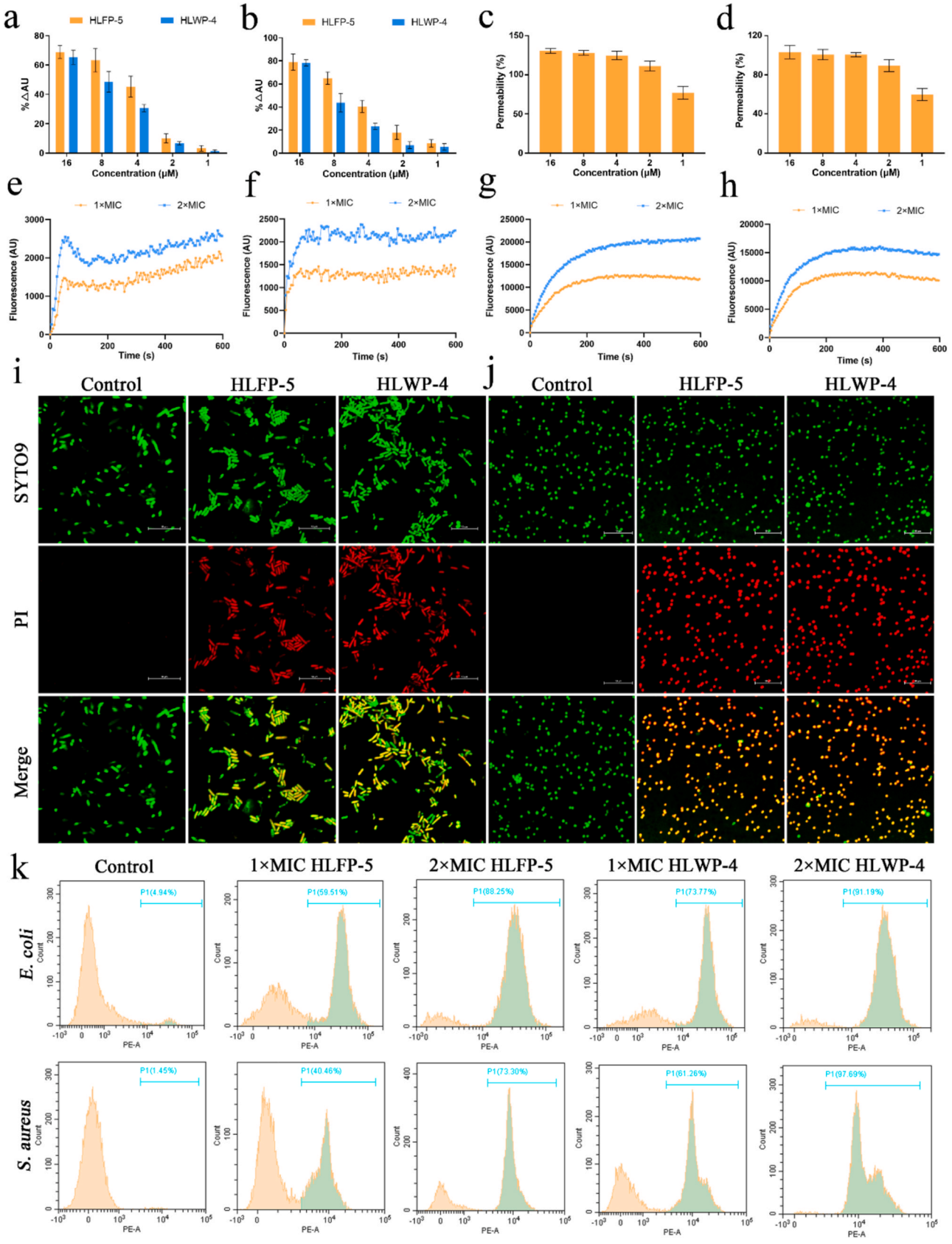

Fig. 3. a, b) Binding capacity of target peptides HLFP-5 and HLWP-4 to a) lipopolysaccharide from *E. coli* or b) lipoteichoic acid from *S. aureus*. c, d) Permeability of the target peptides c) HLFP-5 or d) HLWP-4 to the outer membrane of *E. coli*. e, f) Depolarization cytoplasmic membrane of *E. coli* induced by target peptides e) HLFP-5 and f) HLWP-4. g, h) Depolarization cytoplasmic membrane of *S. aureus* induced by target peptides g) HLFP-5 and h) HLWP-4. i, j) Live/dead fluorescence image of i) *E. coli* and j) *S. aureus* treated with 2 ×MIC HLFP-5 or HLWP-4. k) PI positive cells of *E. coli* or *S. aureus* treated with peptides HLFP-5 and HLWP-4 were detected by flow cytometry.

hydrophobicity to exert their antimicrobial activity. However, the C-terminus of positively charged amino acids (Lys and Arg) are recognized and cleaved by trypsin. For hydrophobic amino acids, the C-terminus of aromatic hydrophobic amino acids (Trp, Phe, and Tyr) are specifically recognized and cleaved by chymotrypsin, while aromatic amino acids and other hydrophobic amino acid (such as Leu) are also recognized and cleaved by pepsin [23]. To systematically and comprehensively avoid the hydrolysis of AMPs by the above three proteases, the cleavage sites of pepsin, trypsin, and chymotrypsin were comprehensively considered in the design. Pro contains a pyrrole ring with a complex steric structure that prevents cleavage by proteases, soplacing Pro at the C-terminus of amino acids sensitive to trypsin and chymotrypsin can effectively prevent cleavage. [19]. As shown in Fig. 2a, since the positively charged amino acids (Lys) in the peptide chain were protected by Pro, the antibacterial activity of all engineered peptides did not change after incubation with 8 mg/mL trypsin. Similarly, the aromatic hydrophobic amino acids (Phe or Trp) were also protected by Pro, so the antibacterial ability of the peptides HLFP-4, HLFP-5, and HLWP-4 were not affected by 2 mg/mL chymotrypsin. In contrast, peptides HIFP-4, HIFP-5, and HIWP-4 were completely inactive after incubation with 2 mg/mL chymotrypsin, because His residues were slightly affected by chymotrypsin, and HI is more sensitive to chymotrypsin than HL [23]. Pepsin mainly recognizes hydrophobic amino acids. In the hydrophobic unit, the C-terminus of aromatic amino acids (Phe or Trp) is protected by His and the N-terminus is protected by Pro, and the Leu is protected by Pro, Ile and Lys themselves will not be cleaved by pepsin, therefore, the bioactivity of the engineered peptide does not change after incubation with 8 mg/mL pepsin. Therefore, among the above six peptides, peptides HLFP-5 and HLWP-4 exhibited strong salt and protease stability. Although the antibacterial activity of the target peptides HLFP-5 and HLWP-4 did not change after co-incubation with proteases, the activity test method does not precisely determine the proportion of the peptides HLFP-5 and HLWP-4 that are cleaved. Therefore, RP-HPLC was used to further determine the proteolytic stability of the peptides. As shown in Fig. 2c–h, peptides HLFP-5 and HLWP-4 did not change in peak area and shape after treatment with 8 mg/mL trypsin or 2 mg/mL chymotrypsin compared to the control. Similarly, the peak area and peak shape of the peptide HLFP-5 did not change significantly after 8 mg/mL pepsin treatment. In contrast, after the peptide HLWP-4 was treated with pepsin, an extra peak appeared, indicating that the peptide HLWP-4 would be slightly cleaved, and the cleavage rate was calculated to be less than 10 % (Fig. 2f). Therefore, the antibacterial activity of the peptide HLWP-4 was not significantly affected by pepsin. (Fig. 2a). In conclusion, the above results indicate that the target peptides have strong proteases stability and can retain their original antibacterial activity at close to the protease concentration in the gastrointestinal tract, and their tolerance to proteases is far stronger than the previously reported natural antibacterial peptide (melittin) [22].

The predominant mechanism of action of peptides

According to the original design intention of cationic and hydrophobicity, we hypothesized that the main action mechanism of engineered peptides is the interaction with bacterial membranes. To make the action mechanism of the peptides more detailed, we selected the target peptides HLFP-5 and HLWP-4 obtained in the previous assays to conduct quantitative and qualitative analysis from outside to inside for gram-negative *E. coli* ATCC25922 and gram-positive *S. aureus* ATCC6538.

The outer membrane containing lipopolysaccharide (LPS) is a unique component of Gram-negative bacteria, the presence of LPS and the outer membrane provides additional protection for Gram-negative bacteria [28]. The premise of AMPs to exert an antibacterial effect is to generate electrostatic interaction with the membrane of bacteria [35]. For Gram-negative bacteria, the outermost component is LPS, so the interaction of the peptides with LPS were determined. BODIPY-TR-cadaverine (BC) fluorescent probe can bind to LPS, resulting in fluorescence quenching. After the peptide binds to LPS, the BC fluorescent probe is displaced, and the fluorescence is released in the solution. As shown in Fig. 3a, the peptides HLFP-5 and HLWP-4 bind to LPS in a concentration-dependent manner, and the binding capacity of the peptide to LPS was about 50 % at 2 × MIC concentration. The main components of Gram-positive bacterial envelopes include peptidoglycan, lipoteichoic acid (LTA), *etc.*, which have also been shown to interact with AMPs [36,37]. Similar to the LPS of Gram-negative bacteria, a unique component of LTA on the surface of Gram-positive bacteria, also showed dose-dependent binding to the peptides (Fig. 3b). This indicates that the higher the concentration of the peptides, the stronger the binding ability to the negatively charged components on the bacterial membrane. *N*-phenyl-1-naphthylamine (NPN) is a hydrophobic probe that fluoresces once the outer membrane of Gram-negative bacteria is loosened and NPN enters the hydrophobic environment inside the cell [38]. As shown in Fig. 3c, d, peptides HLFP-5 and HLWP-4 have very high permeability to the outer membrane of *E. coli*, and at high concentrations, the permeabilization rate of peptide HLFP-5 to the outer membrane of *E. coli* even exceeds 100 %, indicating the ability to destroy the outer membrane stronger than of polymyxin B. The positive charge of the peptide determines the binding ability to the negative charge of the bacterial membrane, and the hydrophobicity determines the ability to destroy the bacterial membrane [39]. As expected, the overall hydrophobicity of peptide HLFP-5 was stronger than that of peptide HLWP-4, and thus the ability of peptide HLFP-5 to induce permeabilization of the outer membrane of Gram-negative bacteria was also greater. The cytoplasmic membrane is considered to be the last line of defense for bacteria, therefore, the cytoplasmic membrane potential changes of *E. coli* ATCC25922 and *S. aureus* ATCC6538 after peptide treatment were measured using the cytoplasmic membrane-sensitive dye DiSC3(5). As shown in Fig. 3e-h, *E. coli* and *S. aureus* cytoplasmic membranes were strongly and rapidly depolarized after treatment with peptides HLFP-5 and HLWP-4. For *E. coli*, the release of fluorescence reaches a maximum at around 50 s, while it takes about 200 s for *S. aureus* to reach a maximum. This may be because the peptidoglycan of *S. aureus* is much thicker than that of *E. coli*, and the peptidoglycan layer hinders the speed of AMPs reaching the cytoplasmic membrane to a certain extent. These data reveal that the high stability peptides HLFP-5 and HLWP-4 exert antibacterial effects by perturbing bacterial membranes.

To further qualitatively and quantitatively study the antibacterial mechanism of the peptides, the membrane permeable dye SYTO9 and the non-membrane permeable dye propidium iodide (PI) were used to perform fluorescence imaging analysis of the peptide-treated bacteria. As shown in Fig. 3i, j, the membrane without peptide treatment is intact, SYTO9 fluoresces green across the intact cell membrane to bind to DNA, PI cannot enter the cell and combine with DNA. Consistent with previous research results, the cytoplasmic membranes of *E. coli* and *S. aureus* treated with peptides were ruptured, and PI entered the cells and chimeric into DNA to emit red fluorescence and overlapping with green fluorescence. (Fig. 3i, j) [40]. Based on the above results, the proportion of dead cells was analyzed with flow cytometry. 1 ×MIC of peptides HLFP-5 and HLWP-4 induced mild bacterial death, and doubling the concentration would cause a large number of bacterial death, and the bacterial death ratio was close to or even more than 90 % (Fig. 3k). To make the bactericidal procedure of the target peptide more transparent, the bactericidal kinetics of the peptides were determined using a standardized protocol (Fig. 4b). The results of bactericidal kinetics showed that peptides HLFP-5 and HLWP-4 had similar bactericidal rates (Fig. 4c–f). Specifically, at 1 ×MIC concentration,

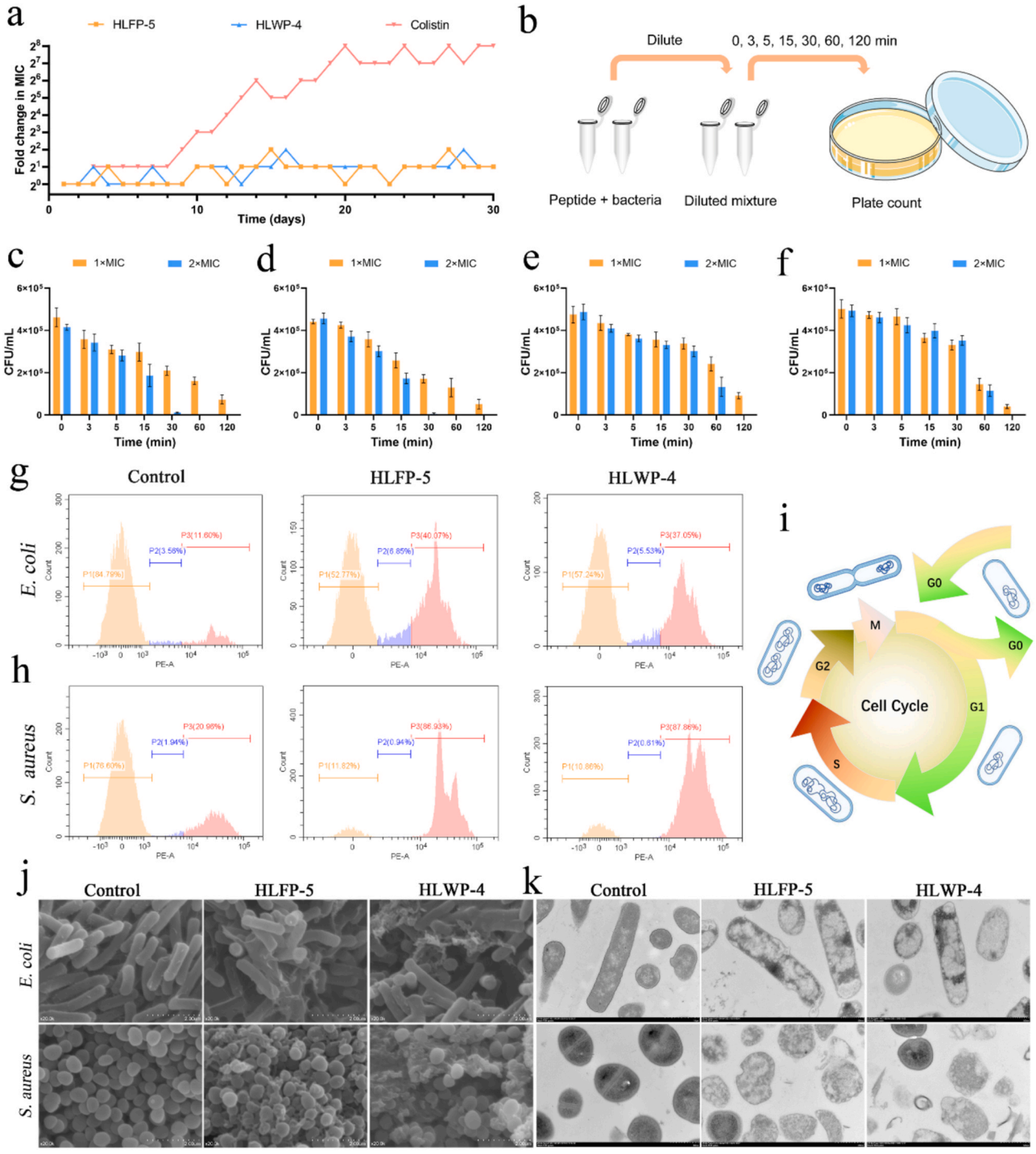

Fig. 4. a) Resistance of the peptides HLFP-5, HLWP-4, and colistin to *E. coli*. b) Schematic diagram of the killing kinetics assay process. c, d) The killing kinetics of peptides c) HLFP-5 or d) HLWP-4 at 1 ×MIC and 2 ×MIC against *E. coli*. e, f) The killing kinetics of peptides e) HLFP-5 or f) HLWP-4 at 1 ×MIC and 2 ×MIC against *S. aureus*. g, h) Effects of peptides HLFP-5 and HLWP-4 on the cell cycle of g) *E. coli* or h) *S. aureus*. i) Schematic diagram of the cell cycle of bacteria. j) SEM or k) TEM images of bacteria without peptide treatment and after treatment with 2 ×MIC peptides HLFP-5 or HLWP-4.

peptides HLFP-5 and HLWP-4 could not completely kill *E. coli* and *S. aureus* (Fig. 4c–f). At 2 ×MIC concentration, *E. coli* was completely killed in about 30 min, and *S. aureus* was completely killed in 120 min (Fig. 4c–f). It is speculated that because the peptidoglycan of Gram-positive bacteria is much thicker than that of Gram-negative bacteria, it affects the penetration rate of the peptide. Therefore, the speed of peptides killing Gram-positive bacteria is slower than that of Gram-negative bacteria.

In addition to the direct destruction of bacterial membranes, AMPs have intracellular targets [41]. The division cycle of bacteria is similar to that of eukaryotic cells (Fig. 4i). For example, a bacteriocin lactocin XN8-A can induce bacterial cell cycle arrest and produce antibacterial ability [42]. Inspired by these studies, we investigated the ability of the peptides HLFP-5 and HLWP-4 to interfere with the cell cycle of *E. coli* and *S. aureus*. As shown in Fig. 4g, h, for *E. coli*, cells in G2/M or S phase were significantly increased after peptide treatment, and cells in the G1 phase were decreased, indicating that

the peptide-induced *E. coli* cell cycle arrest in G2/M or S phase. For *S. aureus*, cells in G1 and S phases decreased after peptide treatment and increased in G2/M. Thus, the peptides HLFP-5 and HLWP-4 have similar mechanisms against Gram-negative and Gram-positive bacteria. Furthermore, in drug resistance assay, the antibacterial ability of colistin decreased by 128-256 fold during a passage for 30 consecutive days, while the antibacterial ability of the target peptides HLFP-5 and HLWP-4 hardly changed (Fig. 4a). Therefore, under the action of a comprehensive mechanism, the target peptide is less likely to develop drug resistance than antibiotics.

Based on the above findings, we used scanning electron microscopy (SEM) and transmission electron microscopy (TEM) to directly observe the ultrastructural changes of bacteria to further determine the disruptive effect of the peptides. As anticipated, the results of SEM showed that the originally smooth bacteria became rough, wrinkled, and even broken after treatment with peptides HLFP-5 or HLWP-4 at 2 × MIC (Figure 4j). Furthermore, under TEM, the control bacteria had intact membrane structures and a dense cytoplasm, and the peptide-treated samples showed cytoplasmic vacuoles, membrane ruptures, and leakage of contents (Figure 4k). Collectively, these results demonstrate the process of membrane disruption from the outside to the inside of the high stability peptides HLFP-5 and HLWP-4, including binding negatively charged components of bacterial membranes, altering outer membrane permeability, inducing cytoplasmic membrane depolarization, inducing bacterial membranes rupture, and interfere with the cell cycle, *etc.*

In vivo biocompatibility of target peptides HLFP-5 and HLWP-4

In the previous results, we have demonstrated that the target peptides HLFP-5 and HLWP-4 are not significantly cytotoxicity to IPEC-1 at high concentrations, and to ensure the safety of the treatment, the toxicity of the peptides was further evaluated *in vivo*. Most of the previous studies used rodents as a model to evaluate the *in vivo* effects of drugs, and although the test was simple and easy to operate, some studies failed at the bedside [43]. Considering that pigs as an experimental animal, their anatomy and physiology are close to those of humans, the pig and human genomes are similar in their functional and structural comparison of immune-related proteins, and pigs will spontaneously succumb to infections similar to human disease, they are more suitable for the modeling of treatments for bacterial infections [44]. On that account, the *in vivo* biocompatibility of the peptides HLFP-5 and HLWP-4 was assessed by intraperitoneal injection to weaned piglets at different doses (2.5 mg/kg and 5 mg/kg). The relevant indicators and pathological changes in the liver and kidney can well reflect the biocompatibility of drugs. Peptides HLFP-5 and HLWP-4 were injected intraperitoneally into weaned piglets at low doses (2.5 mg/kg) or high doses (5 mg/kg), and after a 12 h observation period, the organs of the liver and kidney of piglets were calculated relative organ weights changes (Fig. 5a). As shown in Fig. 5b, c, there were no significant differences in relative organ weights of piglets between groups after the observation period. Additionally, parameters related to renal function including creatinine (CREA), urea (UREA), uric acid (Ua), and liver function include alanine aminotransferase (ALT), aspartate aminotransferase (AST), total bilirubin (TBIL), and alkaline phosphatase (ALP) were not significantly different from those in the control group (Fig. 5d–j), indicating that the liver and kidney-related indexes of piglets were maintained at normal levels after treatment with peptides HLFP-5 and HLWP-4. The results of histological images showed no histological abnormalities in the liver and kidney of piglets after low-dose and high-dose treatment with peptides HLFP-5 and HLWP-4 (Fig. 5k). Based on the above results, it is shown that after a single intraperitoneal injection of the peptides HLFP-5 and HLWP-4 into piglets, there is no abnormality in each index, indicating that both peptides have good biocompatibility and can be used to treat bacterial infections in piglets.

In vivo activity of target peptides HLFP-5 and HLWP-4

Based on previous *in vivo* biocompatibility results, 2.5 mg/kg and 5 mg/kg were determined to be safe doses for the peptides HLFP-5 and HLWP-4. Furthermore, previous results indicated that the peptides HLFP-5 and HLWP-4 possess excellent antibacterial activity and stability. Encouraged by these results, the peptides HLFP-5 and HLWP-4 were used for *in vivo* activity assessment. As shown in Fig. 6a, each piglet was injected intraperitoneally with 15 mL of *E. coli* (OD_{600} =0.15), and then waited for 2 h for the bacterial fluid to be completely absorbed by the peritoneum. Subsequently, piglets were treated with a single-dose injection of saline, the peptides HLFP-5 (2.5 mg/kg), or HLWP-4 (2.5 mg/kg). Compared with the saline treatment group, the bacterial load in the liver, kidney, spleen, and lungs of piglets treated with peptides HLFP-5 and HLWP-4 was significantly reduced (Fig. 6b–e). In addition, the antibacterial effect of HLFP-5 on the kidney and lung was significantly better than that of HLWP-4, which may be due to the antibacterial ability against *E. coli*, and the stability of HLFP-5 was better than HLWP-4. Additionally, as a Gram-negative bacteria, *E. coli* releases endotoxins that easily trigger changes in inflammatory factors, which in turn induce shock [45]. AMPs have the ability to neutralize endotoxins thanks to their cationic properties. As shown in Fig. 6f–h, the levels of serum proinflammatory factors TNF-α, IL-6, and IL-1β in piglets treated with peptides HLFP-5 and HLWP-4 were significantly lower than those in the saline-treated group. Furthermore, piglet organs were used for H&E staining analysis. The liver, kidney, spleen, and lung in the saline-treated group showed obvious tissue damage, with bleeding spots and inflammatory tissue infiltration (Fig. 6i). In contrast, tissue damage was significantly reduced after treatment with peptides HLFP-5 and HLWP-4 (Fig. 6i). The above results indicate that the highly stable engineered peptides HLFP-5 and HLWP-4 have good antibacterial effects *in vivo*, and have the potential to treat bacterial infections and inhibit the up-regulation of inflammatory factors.

Conclusion

In this study, high salt and protease hydrolytic stability AMP template $(KP)_3(HYXP)_n(KP)_3\text{-}NH_2$ (X = Trp or Phe, Y = Ile or Leu, n = 2, 3, 4, 5 or 6) was developed and a 20-member library was deduced. The target peptides HLFP-5 and HLWP-4 were filtered out by screening system, which showed broad-spectrum antibacterial activity, low cytotoxicity, and high stability. Furthermore, HLFP-5 and HLWP-4 can significantly relieve the organ bacterial load and reduce the level of inflammatory factors in systemically infected piglets *in vivo*, which exerted antibacterial ability *via* inducing bacterial membrane rupture and interfering with the cell cycle. Theoretically, AMPs composed of natural amino acid sequences can be massively produced *via* genetic engineering and fermentation engineering, which drastically reduce the production cost. In summary, these findings may provide valuable references and theoretical models for designing high stability AMPs, and lay the foundation for further advancing the clinical translation of antibiotic replacement biomaterials and the development of feed substitute antibiotics in animal husbandry.

Experimental section

Peptide synthesis

The designed peptides were synthesized by GL Biochem (Shanghai) Ltd. and purified by reversed-phase high-performance

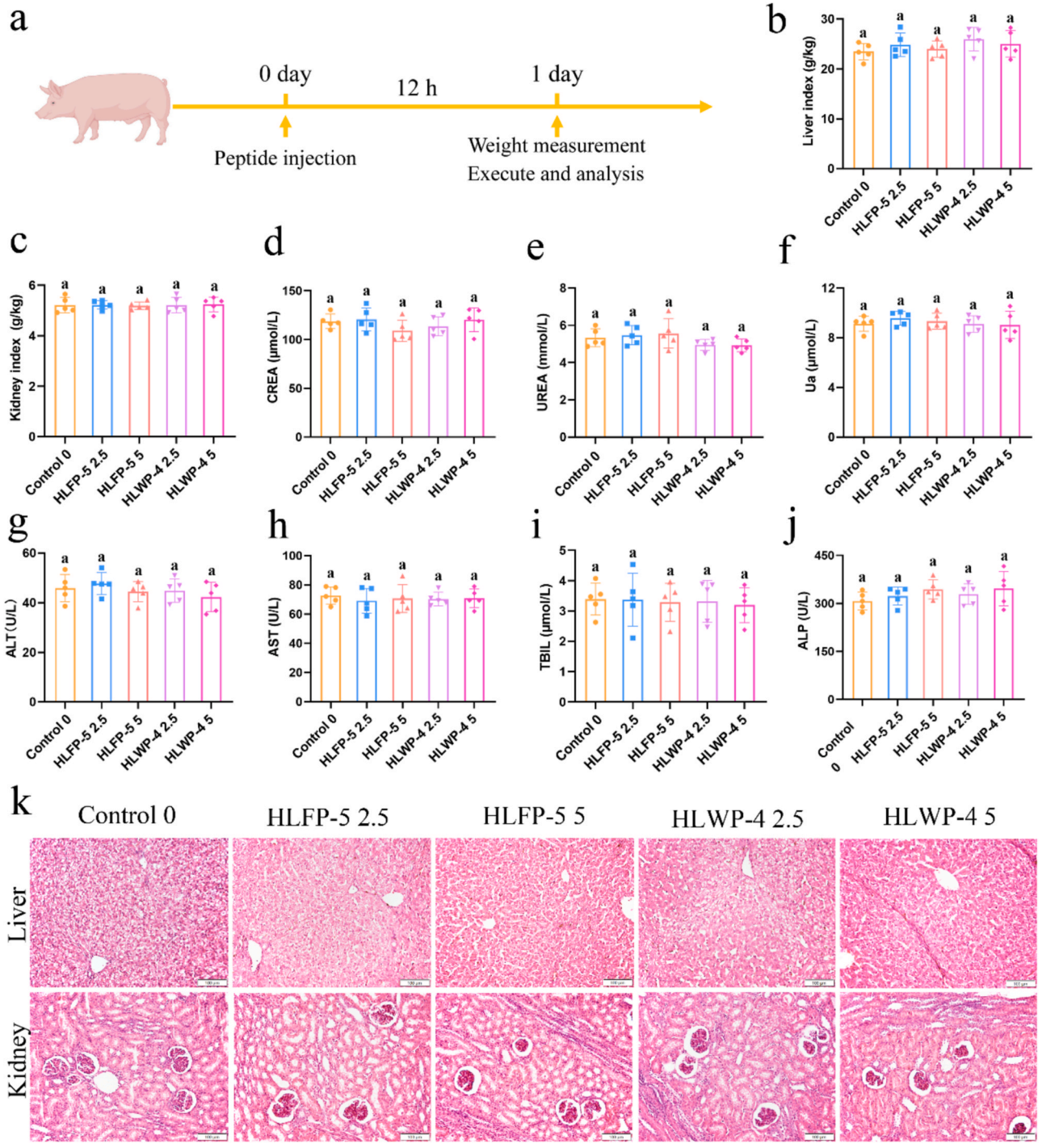

Fig. 5. a) Schematic of the *in vivo* toxicity assay process. b, c) Relative organ weights of b) liver and c) kidney of piglets treated with saline, peptides HLFP-5, or HLWP-4. d-j) Liver- and kidney-related functional parameters in piglet serum. k) Histopathological morphology of liver and kidney of piglets treated with saline, peptides HLFP-5, or HLWP-4.

liquid chromatography (RP-HPLC) to a purity exceeding 95 %. The fidelity and precise molecular masses of the peptides were measured by matrix-assisted laser desorption/ionization time-of-flight mass spectrometry (MALDI-TOF-MS).

Antibacterial activity assay

The MICs of AMPs were determined by the microdilution assay [46]. The bacteria were cultured in Mueller-Hinton broth (MHB) medium to logarithmic growth phase, and then the concentration of the bacterial solution was adjusted to OD_{600} = 0.4 using a spectrophotometer. The adjusted bacterial suspension was diluted 1000-fold with MHB medium. Peptide solutions were serially fold-diluted with bovine serum albumin (BSA) solution (BSA, 0.2 %; acetic acid, 0.01 %) in 96-well plates so that the concentration of peptide amphiphiles was in the range of 0.25–128 μM. The peptide solution was then mixed 1:1 with the diluted bacterial suspension and incubated at 37 °C for 18–24 h. The MIC value was defined as the concentration at which the absorbance measured with a microplate reader at 492 nm was less than 0.1. The assay was repeated three times independently.

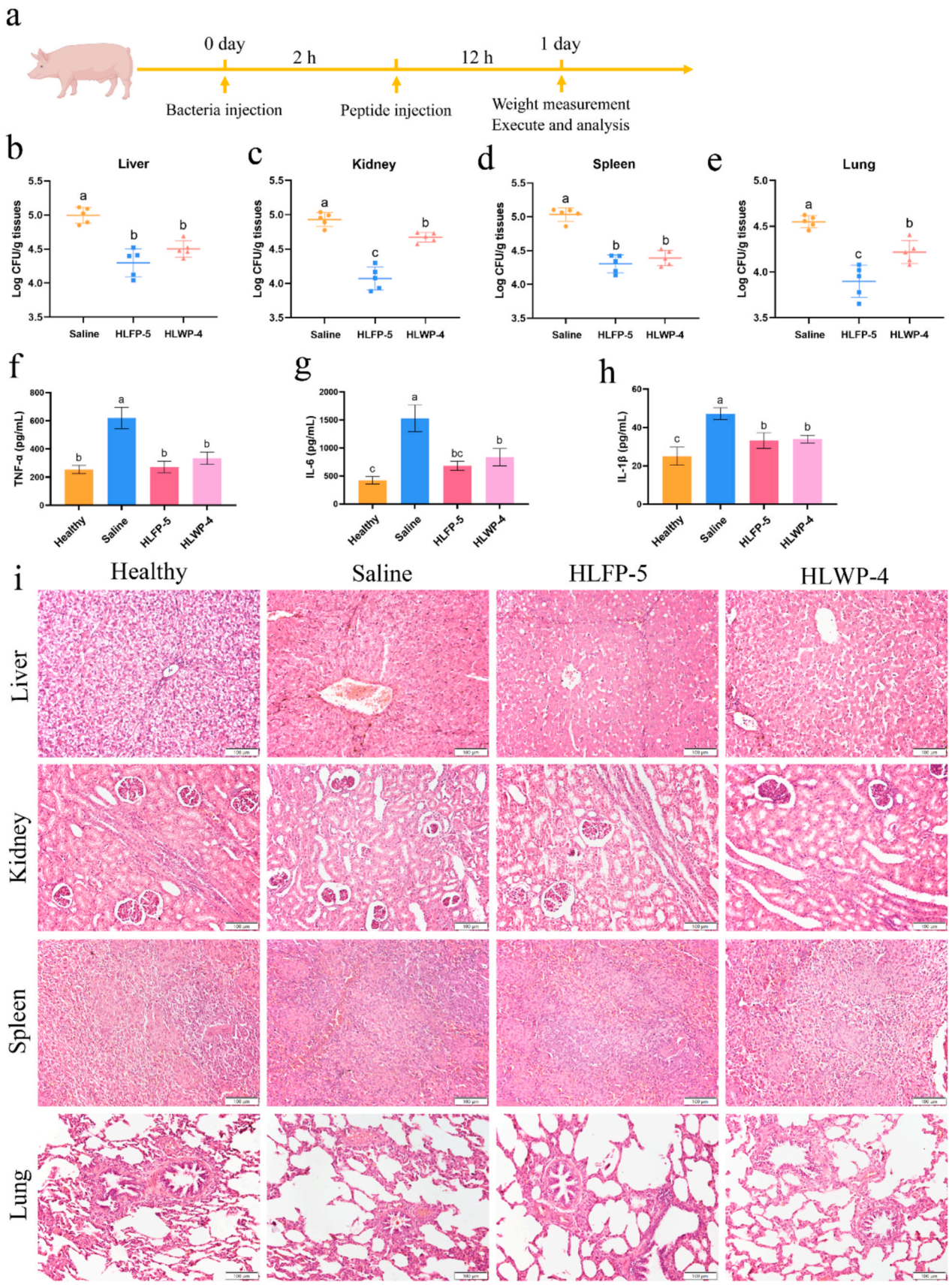

Fig. 6. a) Schematic of the *in vivo* activity assay process. b-e) Bacterial load in organs of infected piglets after treatment with saline, peptides HLFP-5, or HLWP-4. f-h) Serum levels of TNF-α, IL-6, and IL-1β in healthy piglets and *E. coli*-infected piglets treated with saline, peptides HLFP-5, or HLWP-4. b-h) The values with different superscripts (a, b, c) indicate a significant difference ($P < 0.05$). i) H&E staining of organs of healthy piglets and infected piglets treated with saline, peptides HLFP-5, or HLWP-4.

Cytotoxicity assay

The cytotoxicity of AMPs was determined by 3-(4,5-dimethylthiazol-2-yl)-2,5-diphenyltetrazolium bromide (MTT) assay [47]. IPEC-1 cells suspended in DMEM/F12 complete medium (containing 10 % fetal bovine serum) were added to wells 1–11 of 96-well plates at a concentration of 2×10^5 cells/well. Then, place the 96-well plate in a cell culture containing a 5 % CO_2 incubator for 24 h at 37 °C. After discarding the medium, concentrations were varied from 2-128 μM of peptides were added to wells 1–10 of a 96 well plate, medium without peptides was added to well 11 as the positive control, and well 12 containing only medium (without cells) as the negative control. After 4 h of incubation in the incubator, 20 μL MTT (0.5 mg/mL) was added to each well of a 96-well plate and incubated for an additional 2 h. The solution in each well was replaced with 150 μL of DMSO to dissolve the formazan crystals. The absorbance at 570 nm was recorded. The results were calculated as cell viability (%). The assay was repeated three times independently.

Salt stability assay

To determine the effect of salt on the antimicrobial activity of AMPs, the MIC of AMPs in the presence of salt (150 mM NaCl, 4.5 mM KCl, 6 μM NH_4Cl, 8 μM $ZnCl_2$, 1 mM $MgCl_2$, and 4 μM $FeCl_3$) was determined. The assay was repeated three times independently.

Circular dichroism spectrum

Determination of the secondary structure of AMPs by circular dichroism spectrometer [48]. The circular dichroism spectra of AMPs (final concentration: 50 μM) in 10 mM PBS, 30 mM SDS, or 50 % TFE were determined. The data are expressed as mean residue ellipticity: (observed ellipticity × 1000) / (peptide concentration × path length × number of amino acids).

Protease hydrolytic stability assay

For the MIC method, the changes in antimicrobial activity of AMPs after incubation with different proteases (8 mg/mL pepsin, 8 mg/mL trypsin, or 2 mg/mL chymotrypsin) were determined [49]. AMPs (2560 μM) were mixed with protease 1:1 (v/v), and their antibacterial activity was measured according to the method mentioned above after incubation at 37 °C for 8 h. The assay was repeated three times independently.

For the HPLC method, after mixing equal volumes of AMPs (2560 μM) with protease (8 mg/mL pepsin, 8 mg/mL trypsin, or 2 mg/mL chymotrypsin) and incubating at 37 °C for 0 or 8 h. Samples were diluted with ultrapure water to a final peptide concentration of 256 μM. Then, the samples were heated at 100 °C for 5 min to inactivate the proteases. The samples were analyzed using an RP-HPLC system equipped with an Acchorm Unitary C18 column (5 μm, 100 Å, 4.6 mm × 250 mm). Acetonitrile and water solution containing 0.1 % trifluoroacetic acid were used as mobile phases at a flow rate of 1 mL/min. Adjust the loading amount of each sample to make the sample peaks appear more obvious. The absorbance unit (AU) at 220 nm was recorded.

LPS and LTA binding assay

The binding affinity of the peptides to LPS from *E. coli* or LTA from *S. aureus* was determined by fluorescent probe BODIPY-TR-cadaverine (BC) [50]. Fluorescent probe BC (5 μg/mL) mixed with LPS (50 μg/mL) or LTA (50 μg/mL) in Tris buffer (50 mM, pH = 7.4) incubated for 4 h at 37 °C. Subsequently, the peptides HLFP-5 or HLWP-4 (the final concentration range is 1–16 μM) were added to the mixed solution and incubated for 1 h. Measure fluorescence (excitation λ = 580 nm, emission λ = 620 nm) using a microplate reader. The sample without peptide was used as a negative control, and the sample with a final concentration of 20 μg/mL polymyxin B was added as a positive control, and the results were converted into percentages. The assay was repeated three times independently.

Outer membrane permeability assay

The outer membrane permeability of the peptides HLFP-5 and HLWP-4 to *E. coli* ATCC25922 was determined by the dye NPN [51]. *E. coli* ATCC25922 in logarithmic growth phase were resuspended to OD_{600} = 0.2 in 5 mM HEPES (pH=7.4, containing 5 mM glucose). Then, NPN dye was added to the prepared bacterial suspension at a final concentration of 10 μM. Then, the bacterial suspension was mixed 1:1 (v/v) with the peptide solution (the final concentration range is 1–16 μM) in a 96-well plate. Fluorescence values were measured using a microplate reader at the excitation wavelength of 350 nm and the emission wavelength of 420 nm. An untreated bacterial suspension served as a negative control, and a bacterial suspension treated with 20 μg/mL of polymyxin B served as a positive control. Calculate permeability as a percentage. The assay was repeated three times independently.

Cytoplasmic membrane potential assay

Changes in bacterial cytomembrane potential were measured with the membrane-sensitive dye 3,3'-dipropylthiadicarbocyanine (DiSC3(5)) [52]. *E. coli* ATCC25922 or *S. aureus* ATCC6538 in the logarithmic growth phase were resuspended to OD_{600} = 0.1 in 5 mM HEPES buffer (pH=7.4, containing 40 mM glucose and 200 mM KCl). Subsequently, DiSC3(5) at a final concentration of 0.8 μM was added to the bacterial suspension and incubated in the dark for 90 min. After mixing the bacterial suspension with the peptide solution 1:1 (v/v), the final concentration of the peptide is 1 ×MIC or 2 ×MIC, and the fluorescence change was detected at the excitation wavelength of 620 nm and the emission wavelength of 670 nm using a microplate reader.

Bacterial live/dead staining assay

Bacterial membrane integrity analysis was performed using the nucleic acid dye SYTO9/PI [53]. *E. coli* ATCC25922 and *S. aureus* ATCC6538 cells in the logarithmic growth phase were collected and resuspended to OD_{600} = 0.1 in PBS (10 mM, pH=7.4). Then, the peptides (the final concentration is 2 ×MIC) were mixed 1:1 (v/v) with bacterial suspensions in 96-well plates, and SYTO9 dye at a final concentration of 5 μM and PI dye at a final concentration of 20 μg/mL were added to the samples and incubated at 37 °C for 120 min. The PI dye (P8080) was purchased from Beijing Solarbio Science & Technology Co., Ltd. Images were collected using a laser confocal microscope.

Membrane integrity analysis

Further quantitative analysis of bacterial membrane integrity using flow cytometry. *E. coli* ATCC25922 and *S. aureus* ATCC6538 cells in the same way were used for the membrane integrity analysis. The bacterial suspension was mixed 1:1 (v/v) with the peptides (the final concentration is 1 ×MIC or 2 ×MIC) in a 96-well plate and incubated at 37 °C for 1 h. A final concentration of 20 μg/mL of PI dye was added to each sample. Finally, the data were collected by flow cytometry.

Cell cycle analysis

Cell cycle changes of bacteria were further analyzed using flow cytometry [54]. *E. coli* ATCC25922 and *S. aureus* ATCC6538 cells in the logarithmic growth phase were collected and resuspended to OD_{600} = 0.1 in PBS (10 mM, pH=7.4). The peptides HLFP-5 and HLWP-4 (the final concentration is 1 ×MIC) were added to the bacterial suspension and incubated for 1 h at 37 °C. The bacteria were then collected by centrifugation and 70 % ethanol was added overnight. Then, ethanol was removed by centrifugation, RNase A at a concentration of 200 μg/mL was added and incubated for 1 h at 37 °C. PI dye was added at a final concentration of 20 μg/mL and incubated for 30 min. Finally, the samples were assayed by flow cytometry.

Killing kinetics assay

The killing kinetics assay procedure refers to the previous method [55]. *E. coli* ATCC25922 in the logarithmic growth phase was diluted to OD_{600} = 0.4 and then diluted 1000-fold in PBS (10 mM, pH=7.4). Subsequently, peptides (the final concentration is 1 × MIC or 2 × MIC) were mixed with bacterial suspensions in 1.5 mL tubes for a total of 1 mL. After different time intervals, dilute the mixed solution by an appropriate multiple, and then evenly applied to the Mueller-Hinton agar (MHA) plate. Colonies were counted after overnight incubation at 37 °C. The assay was repeated three times independently.

Resistance development assay

The MICs of the peptides were determined as previously described in the antibacterial activity assay. The drug resistance assay refers to the previous procedure [56]. After 24 h, bacterial suspension was removed from sub-MIC wells and diluted 1000-fold in fresh MHB medium for next-generation MIC testing. The test lasts 30 d, once a day, and records the MIC value for each assay.

SEM and TEM assay

Direct observation of bacterial morphology using SEM and TEM [57]. Bacteria in the logarithmic growth phase were centrifuged and resuspended to OD_{600} = 0.2 in PBS (10 mM, pH=7.4), Subsequently, the bacterial suspension was incubated with the peptides (the final concentration is 2 × MIC) for 2 h at 37 °C. Then, the samples were centrifuged to remove the supernatant, the bacteria were transferred to 1.5 mL tubes, and glutaraldehyde (2.5 %, w/v) was added overnight at 4 °C. The SEM samples and TEM samples were prepared according to the method of Tang et al. [40].

Source of animal and ethics statement

The female weaned piglets (Duroc × Landrace × Large white) were provided by Chongqing Hechuan Dekang Pig Breeding Co., Ltd. All experimental animal procedures were approved by the Animal Care and Use Committee of the China Agricultural University.

In vivo biocompatibility assay

Healthy female weaned piglets (Duroc × Landrace × Large white, weighing ≈ 8 kg) were randomly divided into five groups (5 per group). Piglets were pre-raised for five days to acclimate to the environment. During the experiment, five groups of piglets were injected intraperitoneally with normal saline, low-dose HLFP-5 (2.5 mg/kg), high-dose HLFP-5 (5 mg/kg), low-dose HLWP-4 (2.5 mg/kg) and high-dose HLWP-4 (5 mg/kg), respectively, and the injection volume was 10 mL. 12 h after injection, all piglets were euthanized. After venous blood collection and centrifugation, serum was obtained for blood biochemical index analysis. The kidneys, liver and body weight of piglets were recorded, and some organ samples were fixed with 4 % paraformaldehyde for hematoxylin-eosin (H&E) staining for histological analysis.

In vivo activity assay

Healthy female weaned piglets (Duroc × Landrace × Large white, weighing ≈ 8 kg) were randomly divided into four groups (5 per group). One group of healthy piglets received no treatment and served as a control. Piglets in the other three groups were intraperitoneally injected with 15 mL of *E. coli* ATCC25922 with an OD_{600} = 0.15, and 2 h later, they were given an intraperitoneal injection of saline, peptide HLFP-5 (2.5 mg/kg), or HLWP-4 (2.5 mg/kg), respectively, with an injection volume of 10 mL. After 12 h, all piglets were euthanized. The blood of all piglets was collected and the levels of inflammatory factors in serum were determined by the ELISA method. The inflammatory factor kit was purchased from Shanghai Hengyuan Biological Technology Co., Ltd. Partial livers, kidneys, spleens, and lungs of bacteria-infected piglets were collected for bacterial enumeration studies by standardized localization. Furthermore, some organ samples of piglets were stained with H&E for histological examination.

Statistical analysis

Data are presented as mean ± standard deviation (SD) using GraphPad Prism 8.3.0. Statistical analysis was performed using one-way analysis of variance (ANOVA) followed by Tukey's *post hoc* analysis. $P < 0.05$ was defined as statistically different.

CRediT authorship contribution statement

Peng Tan: Methodology, Validation, Data curation, Writing - original draft. Zhihong Sun, Qi Tang, Shenrui Xu, Tao Wang, Yakun Ding, Huiyang Fu, Chenlong Zhou: Methodology, Data curation, Validation. Yucheng Zhang, Zitian Yue: Validation. Xi Ma: Conceptualization, Visualization, Writing - review & editing, Supervision, Project administration, Funding acquisition.

Data availability

The authors do not have permission to share data.

Declaration of Competing Interest

The authors declare that they have no known competing financial interests or personal relationships that could have appeared to influence the work reported in this paper.

Acknowledgements

This work was supported by the National Key R&D Program of China (2022YFD1300404), the National Natural Science Foundation of China (31930106 and 31829004), the Chinese Universities Scientific Fund (2022TC033), the 2115 Talent Development Program of China Agricultural University (1041-00109019), the Henan Province Public Benefit Research Foundation (201300111200-05), and the 111 Project (B16044).

Appendix A. Supporting information

Supplementary data associated with this article can be found in the online version at doi:10.1016/j.nantod.2023.101793.

References

[1] J. Sun, M. Li, M. Lin, B. Zhang, X. Chen, Adv. Mater. 33 (2021) 2104402.
[2] F. Xie, L. Jiang, X. Xiao, Y. Lu, R. Liu, W. Jiang, J. Cai, Small 18 (2022) 2104885.
[3] N. Mookherjee, M.A. Anderson, H.P. Haagsman, D.J. Davidson, Nat. Rev. Drug Discov. 19 (2020) 311–332.
[4] B.H. Gan, J. Gaynord, S.M. Rowe, T. Deingruber, D.R. Spring, Chem. Soc. Rev. 50 (2021) 7820–7880.
[5] G. Fichman, C. Andrews, N.L. Patel, J.P. Schneider, Adv. Mater. 33 (2021) 2103677.
[6] J. Liu, X. Zhang, P. Zou, J. Yao, L. Liu, Y. Cai, T. Sun, Y. Gao, L.-L. Li, Nano Today 44 (2022) 101505.
[7] M. Zhou, Y. Qian, J. Xie, W. Zhang, W. Jiang, X. Xiao, S. Chen, C. Dai, Z. Cong, Z. Ji, Angew. Chem. Int. Ed. 59 (2020) 6412–6419.
[8] L. Hong, M. Gontsarik, H. Amenitsch, S. Salentinig, Small 18 (2022) 2104211.
[9] Y. Wu, Y. Lin, Z. Cong, K. Chen, X. Xiao, X. Wu, L. Liu, Y. She, S. Liu, R. Zhou, Adv. Funct. Mater. 32 (2022) 2107942.
[10] P. Tan, Q. Tang, S. Xu, Y. Zhang, H. Fu, X. Ma, Adv. Sci. 9 (2022) 2105955.
[11] Y. Qian, S. Deng, Z. Cong, H. Zhang, Z. Lu, N. Shao, S.A. Bhatti, C. Zhou, J. Cheng, S.H. Gellman, J. Am. Chem. Soc. 144 (2022) 1690–1699.
[12] G.B. Qi, D. Zhang, F.H. Liu, Z.Y. Qiao, H. Wang, Adv. Mater. 29 (2017) 1703461.
[13] M. Mamuti, R. Zheng, H.-W. An, H. Wang, Nano Today 36 (2021) 101036.
[14] S.J. Lam, N.M. O'Brien-Simpson, N. Pantarat, A. Sulistio, E.H. Wong, Y.-Y. Chen, J.C. Lenzo, J.A. Holden, A. Blencowe, E.C. Reynolds, Nat. Microbiol. 1 (2016) 1–11.
[15] R. Lei, J. Hou, Q. Chen, W. Yuan, B. Cheng, Y. Sun, Y. Jin, L. Ge, S.A. Ben-Sasson, J. Chen, ACS Nano 12 (2018) 5284–5296.
[16] R. Mourtada, H.D. Herce, D.J. Yin, J.A. Moroco, T.E. Wales, J.R. Engen, L.D. Walensky, Nat. Biotechnol. 37 (2019) 1186–1197.
[17] P. Tan, Z. Lai, Q. Jian, C. Shao, Y. Zhu, G. Li, A. Shan, ACS Appl. Mater. Interfaces 12 (2019) 2129–2144.
[18] C. Shao, Y. Zhu, Q. Jian, Z. Lai, P. Tan, G. Li, A. Shan, Small 17 (2021) 2003899.
[19] J. Wang, J. Song, Z. Yang, S. He, Y. Yang, X. Feng, X. Dou, A. Shan, J. Med. Chem. 62 (2019) 2286–2304.
[20] C.M. Anderson, A. Cardenas, R. Elber, L.J. Webb, J. Phys. Chem. B 123 (2018) 170–179.
[21] Z.Y. Ong, N. Wiradharma, Y.Y. Yang, Adv. Drug Deliv. Rev. 78 (2014) 28–45.
[22] Y. Zhu, C. Shao, G. Li, Z. Lai, P. Tan, Q. Jian, B. Cheng, A. Shan, J. Med. Chem. 63 (2020) 9421–9435.
[23] B. Keil, Specificity of proteolysis, Springer Science & Business Media, 2012.
[24] L.M. Yin, M.A. Edwards, J. Li, C.M. Yip, C.M. Deber, J. Biol. Chem. 287 (2012) 7738–7745.
[25] Z. Ma, D. Wei, P. Yan, X. Zhu, A. Shan, Z. Bi, Biomaterials 52 (2015) 517–530.
[26] Y. Chen, M.T. Guarnieri, A.I. Vasil, M.L. Vasil, C.T. Mant, R.S. Hodges, Antimicrob. Agents Chemother. 51 (2007) 1398–1406.
[27] P. Tan, H. Fu, X. Ma, Nano Today 39 (2021) 101229.
[28] R.M. Epand, C. Walker, R.F. Epand, N.A. Magarvey, Biochim. Et. Biophys. Acta (BBA)-Biomembr. 1858 (2016) 980–987.
[29] L. Shang, Y. Wu, N. Wei, F. Yang, M. Wang, L. Zhang, C. Fei, Y. Liu, F. Xue, F. Gu, ACS Appl. Mater. Interfaces 14 (2022) 1245–1258.
[30] Z. Yang, S. He, J. Wang, Y. Yang, L. Zhang, Y. Li, A. Shan, J. Med. Chem. 62 (2019) 4586–4605.
[31] H. Fedders, M. Michalek, J. Grötzinger, M. Leippe, Biochem. J. 416 (2008) 65–75.
[32] N. Dong, X. Zhu, S. Chou, A. Shan, W. Li, J. Jiang, Biomaterials 35 (2014) 8028–8039.
[33] H.-Y. Yu, B.-S. Yip, C.-H. Tu, H.-L. Chen, H.-L. Chu, Y.-H. Chih, H.-T. Cheng, S.-C. Sue, J.-W. Cheng, Biochim. Et. Biophys. Acta (BBA)-Biomembr. 1828 (2013) 2720–2728.
[34] Y. Di, Q. Lin, C. Chen, R. Montelaro, Y. Doi, B. Deslouches, Sci. Adv. 6 (2020) eaay6817.
[35] J. Li, L. Shang, J. Lan, S. Chou, X. Feng, B. Shi, J. Wang, Y. Lyu, A. Shan, ACS Appl. Mater. Interfaces 12 (2020) 44459–44474.
[36] O.P. Neelay, C.A. Peterson, M.E. Snavely, T.C. Brown, A.F. TecleMariam, J.A. Campbell, A.M. Blake, S.C. Schneider, M.E. Cremeens, J. Mol. Struct. 1146 (2017) 329–336.
[37] P. Tan, Z. Lai, Y. Zhu, C. Shao, M.U. Akhtar, W. Li, X. Zheng, A. Shan, ACS Biomater. Sci. Eng. 6 (2019) 398–414.
[38] W. Yu, J. Wang, Z. Wang, L. Li, W. Li, J. Song, S. Zhang, A. Shan, J. Med. Chem. 64 (2021) 10469–10481.
[39] N. Frederiksen, P.R. Hansen, D. Zabicka, M. Tomczak, M. Urbas, I. Domraceva, F. Björkling, H. Franzyk, ChemMedChem 15 (2020) 2544–2561.
[40] Q. Tang P. Tan Z. Dai T. Wang S. Xu Y. Ding J. Jin X. Zhang Y. Zhang C. Zhou Acta Biomater 157 2023 210 224.
[41] K. Hammond, H. Lewis, S. Halliwell, F. Desriac, B. Nardone, J. Ravi, B.W. Hoogenboom, M. Upton, J.P. Derrick, M.G. Ryadnov, Iscience 23 (2020) 101423.
[42] L. Yi, J. Dang, L. Zhang, Y. Wu, B. Liu, X. Lü, Food Control 67 (2016) 53–62.
[43] R.D. Goldfarb, A. Marton, É. Szabó, L. Virág, A.L. Salzman, D. Glock, I. Akhter, R. McCarthy, J.E. Parrillo, C. Szabó, Crit. Care Med. 30 (2002) 974–980.
[44] L.K. Jensen, N.L. Henriksen, H.E. Jensen, Lab. Anim. 53 (2019) 125–136.
[45] J.L. Narayana, B. Mishra, T. Lushnikova, Q. Wu, Y.S. Chhonker, Y. Zhang, D. Zarena, E.S. Salnikov, X. Dang, F. Wang, Proc. Natl. Acad. Sci., 117 (2020) 19446–19454.
[46] M. Song, Y. Liu, T. Li, X. Liu, Z. Hao, S. Ding, P. Panichayupakaranant, K. Zhu, J. Shen, Adv. Sci. 8 (2021) 2100749.
[47] Y. Fang, Y. Zhu, L. Li, Z. Lai, N. Dong, A. Shan, Small Methods 5 (2021) 2101304.
[48] H. Gong, M.-A. Sani, X. Hu, K. Fa, J.W. Hart, M. Liao, P. Hollowell, J. Carter, L.A. Clifton, M. Campana, ACS Appl. Mater. Interfaces 12 (2020) 55675–55687.
[49] Z. Lai, P. Tan, Y. Zhu, C. Shao, A. Shan, L. Li, ACS Appl. Mater. Interfaces 11 (2019) 22113–22128.
[50] L. Shang, J. Li, C. Song, Z. Nina, Q. Li, S. Chou, Z. Wang, A. Shan, Front. Microbiol. 11 (2020) 1767.
[51] J.Y. Kwon, M.K. Kim, L. Mereuta, C.H. Seo, T. Luchian, Y. Park, AMB Express 9 (2019) 1–15.
[52] Y. Li, F. Liu, J. Zhang, X. Liu, P. Xiao, H. Bai, S. Chen, D. Wang, S.H. Sung, R.T. Kwok, Adv. Sci. 8 (2021) 2001750.
[53] M. Yasir, D. Dutta, M.D. Willcox, Sci. Rep. 9 (2019) 1–12.
[54] L. Li, J. Sun, S. Xia, X. Tian, M.J. Cheserek, G. Le, Appl. Microbiol. Biotechnol. 100 (2016) 3245–3253.
[55] B. Zhang, M. Zhang, M. Lin, X. Dong, X. Ma, Y. Xu, J. Sun, Small 18 (2022) 2106936.
[56] Y. Gao, J. Wang, M. Chai, X. Li, Y. Deng, Q. Jin, J. Ji, ACS Nano 14 (2020) 5686–5699.
[57] X. Qu, M. Wang, M. Wang, H. Tang, S. Zhang, H. Yang, W. Yuan, Y. Wang, J. Yang, B. Yue, Adv. Mater. (2022) 2200096.